Electronic Supplementary Information

From discrete $[Y(DMF)_8][Cu_4(\mu_3\text{-}I)_2(\mu\text{-}I)_3I_2]$ ion pairs to extended $[Y(DMF)_6(H_2O)_2]$ $[Cu_7(\mu_4\text{-}I)_3(\mu_3\text{-}I)_2(\mu\text{-}I)_4(I)]_{1\infty}$ and $[Y(DMF)_6(H_2O)_3][Cu^{I}_7Cu^{II}_2$ $(\mu_3\text{-}I)_8(\mu\text{-}I)_6]_{2\infty}$ arrays by H-bonding templating in a confined solvent-free environment ?

Shashank Mishra,* Liliane G. Hubert Pfalzgraf, Erwann Jeanneau and Henry Chermette

Université Claude Bernard Lyon 1, IRC-UPR 5401, 2 avenue A. Einstein, 69626 Villeurbanne Cédex, France. Email : mishrashashank74@rediffmail.com

Experimental

Synthesis of (**1**) was carried out under argon using Schlenk tubes and vacuum line techniques. CuI (Aldrich) and NH_4I (Sigma-Aldrich) were used as received. $YI_3(Pr^iOH)_4$ was synthesized as described in our recent paper.[1] Solvents were purified by standard methods. Isopropoxyethanol was stored over molecular sieves. ^1H NMR spectrum was registered on a Bruker AC-300 spectrometer. FT-IR spectrum was recorded as Nujol mulls on a Perkin-Elmer Paragon 500 spectrometer. The ESR spectrum (X-band, 9.4 GHz) of (**3**) was measured in DMF at 77 K using a Bruker spectrometer (microwave power of 10 mW and a modulation frequency of 100 kHz). DPPH was used as reference (g = 2.0036). Analytical data were obtained from the Service Central d'Analyses du CNRS.

X-Ray structure determination of (1)-(3)

Crystals of (**1**)-(**3**) were mounted on a Nonius Kappa CCD diffractometer using MoK_α radiation (λ = 0.71073 Å). Intensities were collected at 150 K by means of the COLLECT software.[2] Reflection indexing, Lorentz-polarization correction, peak integration and background determination were carried out with DENZO.[3] Frame scaling and unit-cell parameters refinement were made with SCALEPACK.[3] No absorption corrections were applied, since they did not improve the refinement. The structures of (**1**)–(**3**) were solved by direct methods with SIR97.[4] The remaining non-hydrogen atoms were located by successive difference Fourier map analyses.

The hydrogen atoms were placed geometrically and included in the refinement using soft restraints on the bond lengths and angles to regularize their geometry (C-H in the range 0.93-0.98 Å and O-H = 0.82 Å) and isotropic atomic displacement parameters (U(H) in the range 1.2-1.5 times $U_{eq.}$ of the adjacent atom). The structure refinement was carried out with CRYSTALS.[5] In the structure (**2**), the maximum residual density peak Q1 of 13.75 e.Å^{-3} is located at 1.113 Å from H53. Some other high residual densities are: Q2 of 6.93 e.Å^{-3} at 2.261 Å from Cu1 and Q3 of 4.59 e.Å^{-3} at 1.157 Å from Cu1. For compound (**3**), the maximum residual density peak Q1 of 5.21 e.Å^{-3} is located at 1.50 Å from Q3. Some other high residual densities are: Q2 of 4.93 e.Å^{-3} at 2.49 Å from I2 and Q3 of 3.56 e.Å^{-3} at 1.50 Å from Q1. These high residual electron densities can be explained by the fact that the cluster condensation is dynamic and occurs over time. Indeed, as the structure is continuously evolving, it was not possible to record data of structures (**2**) and (**3**) accurately, especially taking into account the small size of the crystal (0.151 × 0.273 × 0.316). Structures (**2**) and (**3**) are accurate (correct distances, thermal ellipsoids) but their data collections are contaminated by metallic fragments that have not yet or already evolved. We thus tried to find a twinning relation in the data but none fitted the observations made. It is also worth noting that evolution is continuing, (**3**) is not stable but lead to a polycrystalline material. To our knowledge this is the first time that a structural transformation of a moisture-sensitive compound has been observed on a unique crystal by X-Ray diffraction, the paratone medium providing a confined environment for the evolution.

DFT calculations

The density functional theory within the Kohn-Sham methodology[6] has been used to model the three clusters. The generalized gradient approximation (GGA) has been employed within the Perdew-Burke-Ernzerhof (PBE) exchange-correlation functional formulation.[7] The calculations have been performed using the ADF05 program package.[8] The basis set was of triple-ξ quality + polarization (TZP) with small frozen cores. Relativistic effects are expected not to be negligible,

at least for iodine, hence these effects have been taken into account for all electrons with the Zero Order Regular Approximation (ZORA).[9] Finally the integration grid parameter, setting the numerical integration accuracy, has been fixed to 5.

The bond lengths and angles used for copper iodide clusters in (**1**)-(**3**) are taken from single crystal X-ray data (geometry optimizations of the negatively charged clusters would have lead to strong relaxation of the position of link iodine). Mulliken charges of Cu atoms are negative in most cases, because of the anionic charges of the clusters, which are not fully distributed on the iodine atoms. Accordingly, they amount -0.17 ± 0.03 for $Cu_4I_7^{3-}$, -0.22 ± 0.03 for $Cu_7I_{12}^{5-}$, -0.23 ± 0.06 for Cu(I) in $Cu_6I_{13}^{6-}$ and 0.01 for Cu(II) in $Cu_6I_{13}^{6-}$. These values are coherent with both of values expected taking into account the total charge of the cluster, and of Hirshfeld charges[10], although they provide different numerical values (0.00 ± 0.01 for $Cu_4I_7^{3-}$, -0.01 and - 0.03 for $Cu_7I_{12}^{5-}$, -0.04 ± 0.03 for Cu(I) (link atoms) in $Cu_6I_{13}^{6-}$ and 0.13 ± 0.07 for Cu(II)/Cu(I) (triangle) in $Cu_6I_{13}^{6-}$).

References

1 S. Mishra, L. G. Hubert-Pfalzgraf, M. Rolland, H. Chermette, Inorg. Chem. Commun., 10 (2007) 15.

2 B. V. Nonius, *COLLECT*, Nonius, Delft, The Netherlands (1997-2001).

3 Z. Otwinowski and W. Minor, *Methods in Enzymology*, *Vol. 276* (Eds.: C. W. Carter Jr, R. M. Sweet), Academic Press, New York, **1997**, pp. 307--326.

4 A. Altomare, M. C. Burla, M. Camalli, G. L. Cascarano, C. Giacovazzo, A. Guagliardi, A. G. G. Moliterni, G. Polidori and R. Spagna, *J. Appl. Cryst.*, 1999, **32**, 115.

5 D. J. Watkin, C. K. Prout, L. J. Pearce, *CAMERON*, Chemical Crystallography Laboratory, OXFORD, UK (1996).

6 W. Kohn, L. J. Sham, Phys. Rev. 140 (1965) A1133.

7 J. P. Perdew, K. Burke, M. Ernzerhof, Phys. Rev. Lett. 77 (1996) 3865.

8 E.J. Baerends, J. Autschbach, A. Bérces, C. Bo, P. M. Boerrigter, L. Cavallo, D.P. Chong, L. Deng, R. M. Dickson, D. E. Ellis, M. van Faassen, L. Fan, T. H. Fischer, C. Fonseca Guerra, S. J. A. van Gisbergen, J. A. Groeneveld, O. V. Gritsenko, M. Grüning, F. E. Harris, P. van den Hoek,

H. Jacobsen, L. Jensen, G. van Kessel, F. Kootstra, E. van Lenthe, D.A. McCormack, A. Michalak, V. P. Osinga, S. Patchkovskii, P. H. T. Philipsen, D. Post, C. C. Pye, W. Ravenek, P. Ros, P. R. T. Schipper, G. Schreckenbach, J. G. Snijders, M. Sola, M. Swart, D. Swerhone, G. te Velde, P. Vernooijs, L. Versluis, O. Visser, F. Wang, E. van Wezenbeek, G. Wiesenekker, S. K. Wolff, T. K. Woo, A.L. Yakovlev, T. Ziegler: ADF2005.01, SCM, Theoretical Chemistry, Vrije Universiteit, Amsterdam, The Netherlands.

9 E. van Lenthe, E. J. Baerends, and J. G. Snijders, J. Chem. Phys. 99 (1993) 4597; E. van Lenthe, E. J. Baerends, J. G. Snijders, J. Chem. Phys. 101 (1994) 9783; E. van Lenthe, A. E. Ehlers, E. J. Baerends, J. Chem. Phys. 110 (1999) 8943.

10 F.L. Hirshfeld, Theor. Chim. Acta 44 (1977) 129.

Figures

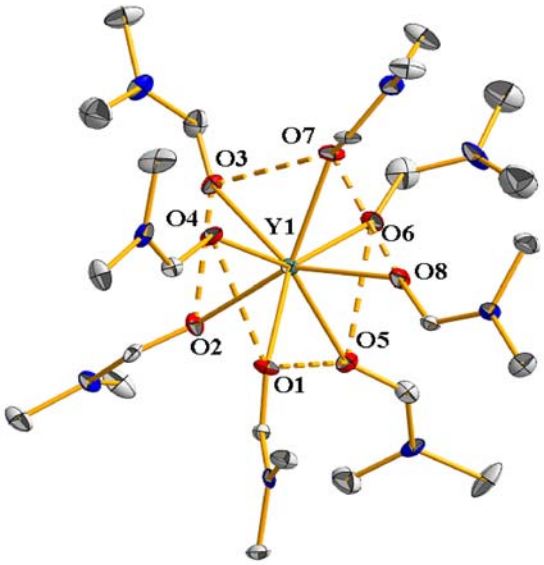

Figure S1. ORTEP view of the $[Y(DMF)_8]^{3+}$ cation of (**1**) with atom labeling and ellipsoids at 30 % probability. Hydrogen atoms from DMF molecules have been removed for clarity. Selected bond lengths (Å) and angles(°): Y1—O1 2.36(6), Y1—O7 2.41(6), O3—Y1—O1 134.4(2), O3—Y1—O2 70.6(2), O3—Y1—O4 79.7(2), O3—Y1—O5 124.3(2), O3—Y1—O6 78.2(2), O3—Y1—O7 72.2(2), O3—Y1—O8 142.6(2).

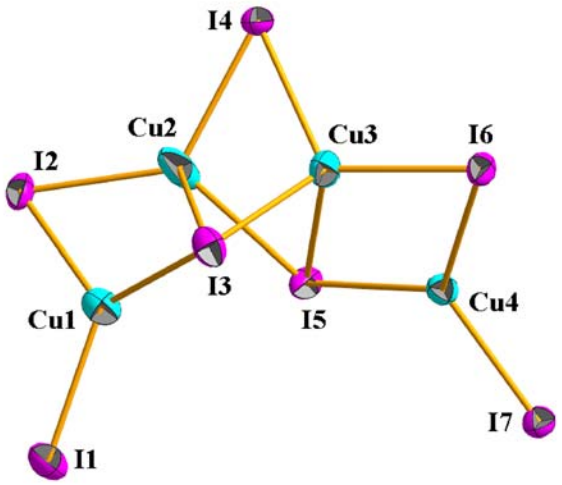

Figure S2. ORTEP view of the $[Cu_4(\mu_3\text{-}I)_2(\mu\text{-}I)_3I_2]^{3-}$ anion of (**1**) with atom labeling and ellipsoids at 30 % probability. Selected bond lengths (Å) and angles(°): Cu1—I1 2.53(1), Cu1—I2 2.56(2), Cu1—I3 2.57(2), Cu2—I3 2.88(2), Cu2—I4 2.64(1), Cu3—I5 2.96(2), Cu1—Cu2 2.69(2), Cu2—Cu3 2.47(2), Cu3—Cu4 2.57(2), I1—Cu1—I2 121.0(5), I1—Cu1—I3 116.1(4), I2—Cu2—I3 111.6(4), I2—Cu2—I4 118.9(6), I3—Cu2—I4 102.1(6), I3—Cu2—I5 98.4(5), I4—Cu2—I5 108.8(5).

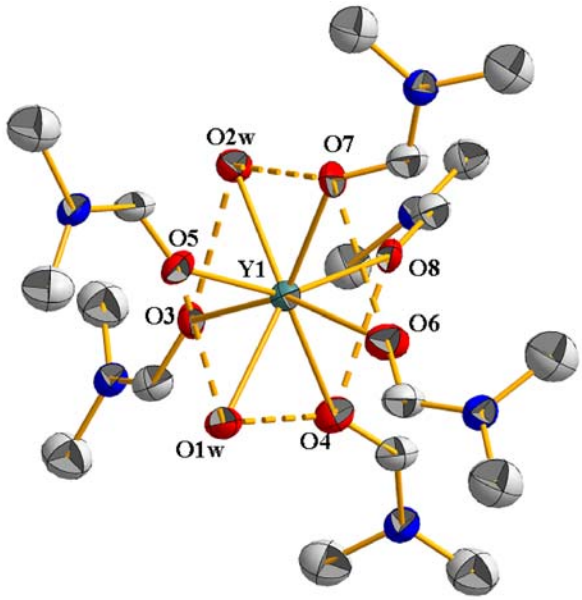

Figure S3. ORTEP view of the $Y(DMF)_6(H_2O)_2]^{3+}$ cation of (**2**) with atom labeling and ellipsoids at 30 % probability. Hydrogen atoms from DMF molecules have been removed for clarity. Selected bond lengths (Å) and angles(°): Y1—O1w 2.42(2), Y1—O8 2.25(2), O1w—Y1—O2w 135.9(7), O3—Y1—O2 69.5(7), O3—Y1—O4 75.0(7), O3—Y1—O5 89.7(3), O3—Y1—O6 151.7(6), O3—Y1—O7 137.6(6), O3—Y1—O8 95.3(7).

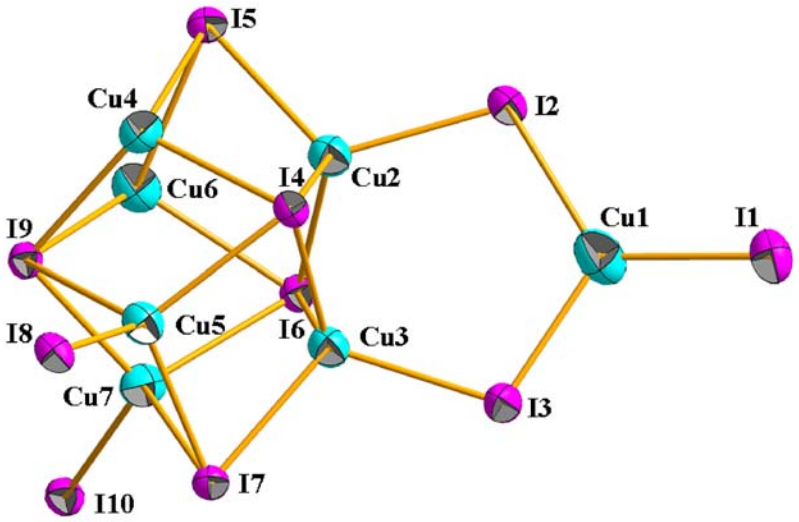

Figure S4. ORTEP view of the $[Cu_7(\mu_4\text{-}I)_3(\mu_3\text{-}I)_2(\mu\text{-}I)_4(I)]^{3-}$ anion of (**2**) with atom labeling and ellipsoids at 30 % probability. Selected bond lengths (Å) and angles(°): Cu1—I2 2.59(7), Cu1—I3 2.55(6), Cu2—I2 2.62(5), Cu2—I4 2.69(5), Cu2—I5 2.65(5), Cu2—Cu3 2.82(6), Cu2—Cu4 3.03(6), Cu2—Cu6 3.20(7), I2—Cu1—I3 116.8(2), I1—Cu1—I2 123.0(2), I1—Cu1—I3 117.9(2), I4—Cu5—I8 112.4(2), I7—Cu5—I8 110.9(2), I7—Cu5—I4 106.2(2), I9—Cu5—I4 111.4(2), I9—Cu5—I7 103.3(2).

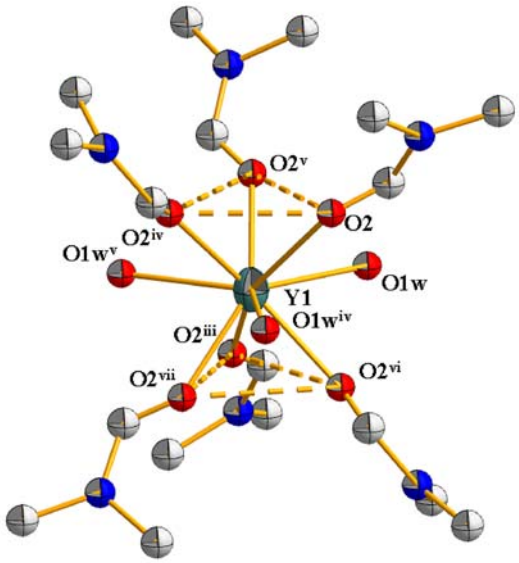

Figure S5.ORTEP view of the $[Y(DMF)_6(H_2O)_3]^{3+}$ cation of (**3**) with atom labeling and ellipsoids at 30 % probability. Hydrogen atoms from DMF molecules have been removed for clarity. Selected bond lengths (Å) and angles(°): Y1—O1w^{iv} 2.52(2), Y1—O2^{iv} 2.34(1), O1w^{iv}—Y1—O1w^{v} 120.0(5), O1w^{iv}—Y1—O2^{iv} 73.5(4), O1w^{v}—Y1—O2^{iv} 65.2(4), O1w^{iv}—Y1—O2^{v} 134.7(4), O2^{iv}—Y1—O2^{v} 75.5(6), O2^{iv}—Y1—O2^{iii} 130.5(8), O2^{v}—Y1—O2^{iii} 90.7(8). Symmetry codes: (i) 1-y, 1+x-y, z; (ii) –x+y, 1-x, z; (iii) 4/3-x, 2/3-x+y, 1/6-z; (iv) –x+y, 2-x, z; (v) 2-y, 2+x-y, z; (vi) y-2/3, 2/3+x, 1/6-z; (vii) 4/3+x-y, 8/3-y, 1/6-z.

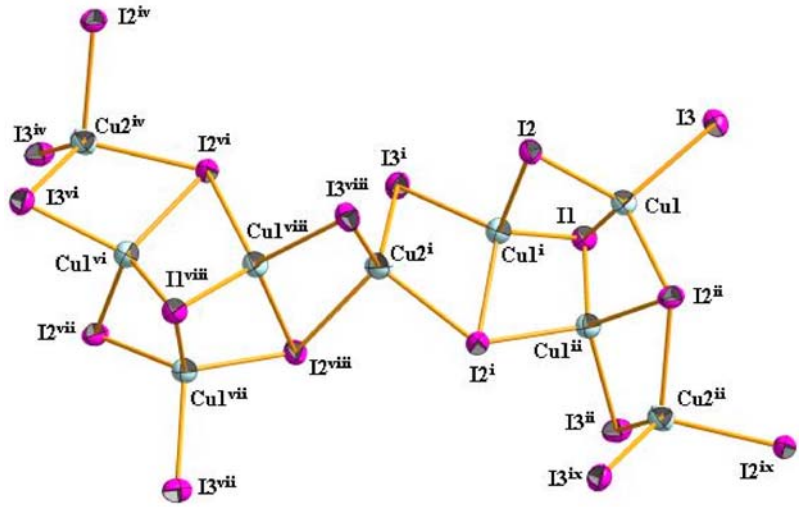

Figure S6. ORTEP view of the $[Cu^{I}_{7}Cu^{II}_{2}(\mu_3\text{-}I)_8(\mu\text{-}I)_6]^{-3}$ anion of (**3**) with atom labeling and ellipsoids at 30 % probability. Selected bond lengths (Å) and angles(°): Cu1—Cu1^{i} 2.79(3), Cu1—Cu1^{ii} 2.79(3), Cu1—Cu2 2.77(2), Cu1—I1 2.66(3), Cu1—I2 2.70(2), I2^{ii}—Cu1—I1 112.5(8), I2^{ii}—Cu1—I2 107.6(1), I1—Cu1—I2 111.5(8), I2^{ii}—Cu1—I3 107.1(8), I1—Cu1—I3 105.6(9), I2—Cu1—I3 112.4(8). Symmetry codes: (i) 1-y, 1+x-y, z; (ii) –x+y, 1-x, z; (iii) 4/3-x, 2/3-x+y, 1/6-z; (iv) –x+y, 2-x, z; (v) 2-y, 2+x-y, z; (vi) y-2/3, 2/3+x, 1/6-z; (vii) 4/3+x-y, 8/3-y, 1/6-z.

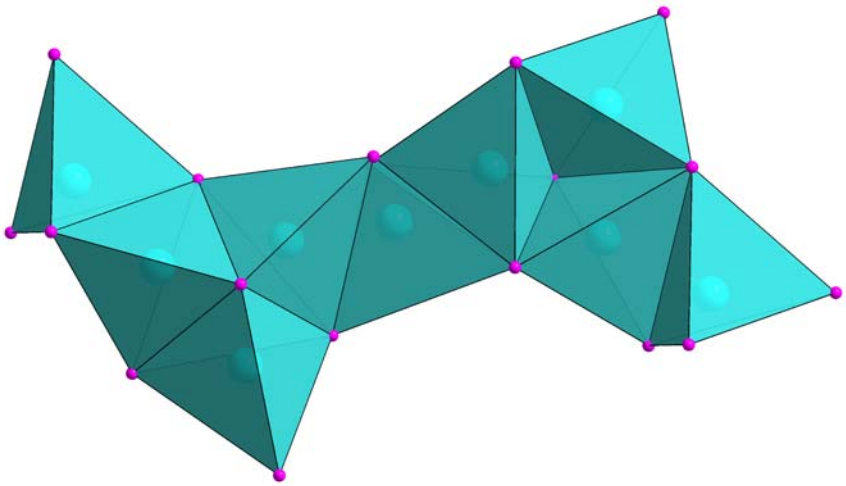

Figure S7. Copper iodide building block $[Cu^{I}_{7}Cu^{II}_{2}(\mu_3\text{-}I)_8(\mu\text{-}I)_6]^{-3}$ for (**3**).

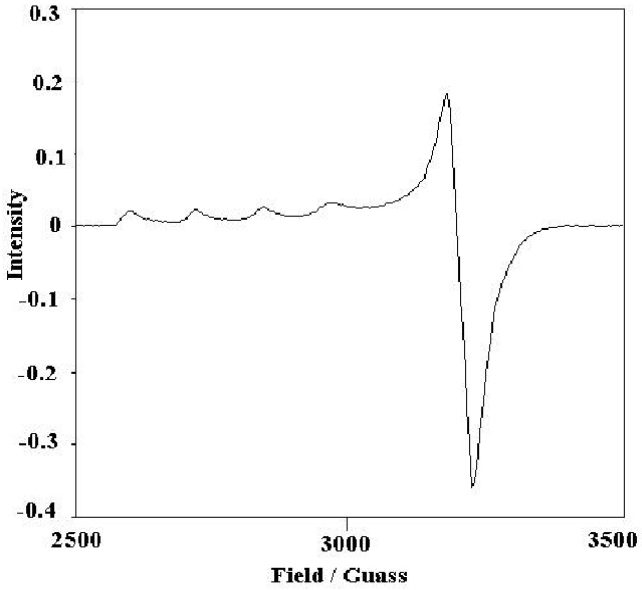

Figure S8. ESR spectrum of $[Y(DMF)_6(H_2O)_3][Cu^{I}_7Cu^{II}_2(\mu_3\text{-}I)_8(\mu\text{-}I)_6]$ (**3**) obtained in frozen DMF solution at 77 K.

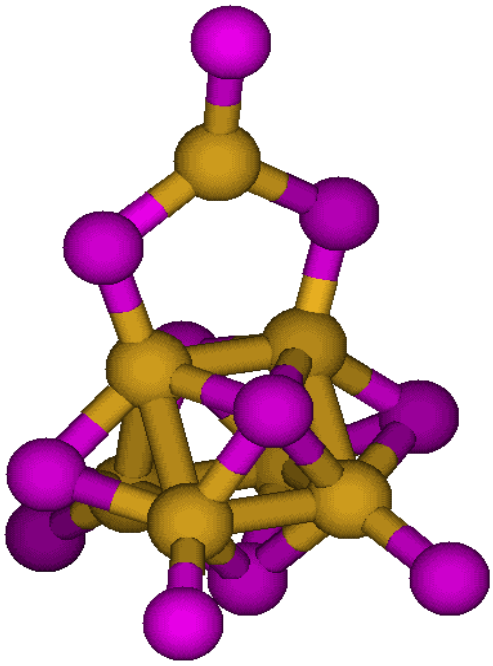

Figure S9. Ball and stick representation of $[Cu^{I}_7I_{12}]^{-5}$ model used for theoretical calculations of 1D copper iodide cluster in (**2**). Atom color designations: copper (brown) and iodine (violet)

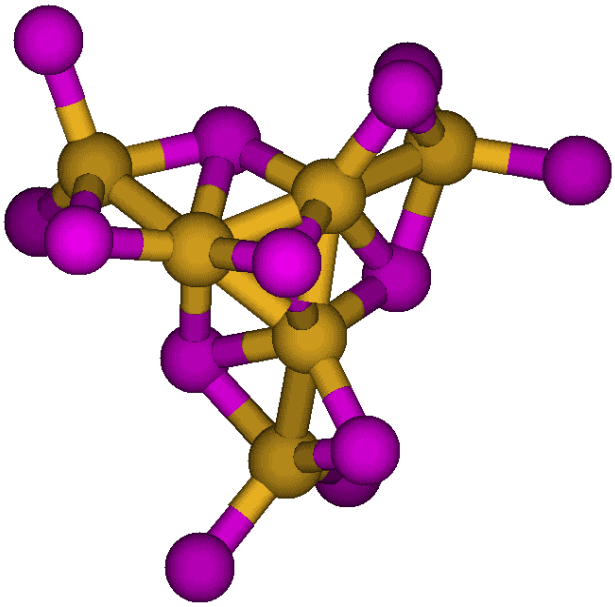

Figure S10. Ball and stick representation of $[Cu^{I}_{5}Cu^{II}I_{13}]^{-6}$ model used for theoretical calculations of 2-D copper iodide cluster in (**3**). Atom color designations: copper (brown) and iodine (violet)